RESEARCH ARTICLE OPEN ACCESS

Small Nuclear Ribonucleoprotein Autoantibody Associated With Blood-Nerve Barrier Breakdown in Guillain-Barré Syndrome

Fumitaka Shimizu,[1] Michiaki Koga,[1,2] Yoichi Mizukami,[3] Kenji Watanabe,[3] Ryota Sato,[1] Yukio Takeshita,[4,5,6] Toshihiko Maeda,[1] Takashi Kanda,[1] and Masayuki Nakamori[1]

Correspondence
Dr. Shimizu
fshimizu@yamaguchi-u.ac.jp

Neurol Neuroimmunol Neuroinflamm 2025;12:e200405. doi:10.1212/NXI.0000000000200405

Abstract

Background and Objectives

Breakdown of the blood-nerve barrier (BNB) is observed in patients with Guillain-Barré syndrome (GBS); however, the molecular mechanism underlying this phenomenon remains unclear.The aim of this study was to identify antibodies against the BNB-endothelial cells that initiate BNB breakdown in patients with GBS.

Methods

We purified IgGs from the serum samples of patients with GBS (n = 77) during the acute phase, disease controls ([DCs], n = 51), and healthy controls ([HCs], n = 24). Human peripheral nerve microvascular endothelial cells (PnMECs) were incubated with IgG. Molecular changes in PnMECs after GBS-IgG exposure were evaluated using RNA-seq and a high-content imaging system. U1-small nuclear ribonucleoprotein (U1-snRNP) autoantibodies were detected using an ELISA. The clinical information of U1-snRNP antibody–positive GBS patients was verified.

Results

GBS-IgGs significantly increased NF-κB nuclear translocation and permeability of the 10-kDa dextran in PnMECs compared with DC-IgGs or HC-IgGs. RNA-seq analyses of PnMECs demonstrated that NF-κB p65 in the center of the network analysis, snRNPs as upstream genes of NF-κB p65, and CXCR5 as downstream genes of NF-κB p65 were important molecules after GBS-IgG exposure. The protein level of claudin-5 and U1-snRNP was significantly reduced while that of CXCR5 was significantly increased after incubation with IgG from patients with GBS, compared with that from HCs. The rate of U1-snRNP antibody positivity was 36% (28 of 77) in patients with GBS, 7% (2 of 28) in DCs, and 0% (0 of 16) in HCs. The serum titer of snRNP antibody decreased after treatment. Both cerebral spinal fluid protein and albumin quotient (QALB)/QALBLIM were higher in snRNP antibody–positive GBS patients than in snRNP antibody–negative GBS patients. IgG from U1-snRNP antibody–positive GBS patients decreased the barrier function and claudin-5 expression more than that from HCs in an in vitro BNB coculture model. The reduction in U1-snRNP antibody decreased the biological effect of IgG from GBS patients with U1-snRNP antibody on the increased permeability of PnMECs.

Discussion

U1-snRNP autoantibodies are associated with the breakdown of BNB in GBS, through the reduction of U1-snRNP and claudin-5 and the induction of NF-κB activation in BNB-endothelial cells. A temporary autoantibody response against snRNP may be boosted by the periodic response to infection in GBS.

MORE ONLINE

Supplementary Material

[1]Department of Neurology and Clinical Neuroscience, Yamaguchi University Graduate School of Medicine, Ube, Japan; [2]Faculty of Medicine and Health Sciences, Yamaguchi University Graduate School of Medicine, Ube, Japan; [3]Center for Gene Research, Yamaguchi University, Ube, Japan; [4]Department of Neurotherapeutics, Yamaguchi University School of Medicine, Ube, Japan; [5]BBB Research Center, Yamaguchi University School of Medicine, Ube, Japan; and [6]Research Institute for Cell Design Medical Science, Yamaguchi University, Ube, Japan.

The Article Processing Charge was funded by the authors.

Glossary

ADEM = acute disseminated encephalomyelitis; **BNB** = blood-nerve barrier; **CIDP** = chronic inflammatory demyelinating polyradiculoneuropathy; **CMV** = cytomegalovirus; **CXCL13** = C-X-C motif ligand 13; **CXCR5** = C-X-C chemokine receptor type 5; **DC** = disease control; **EBV** = Epstein-Barr virus; **FBS** = fetal bovine serum; **FC** = fold-change; **GBS** = Guillain-Barré syndrome; **GDS** = GBS Disability Scale; **HC** = healthy control; **ICAM-1** = intercellular adhesion molecule 1; **IPA** = ingenuity pathway analysis; **IVIg** = IV immunoglobulin; **MCTD** = mixed connective tissue disease; **NFAT** = nuclear factor of activated T cells; **NMOSD** = neuromyelitis optica spectrum disorder; **PBS** = phosphate-buffered saline; **PnMEC** = peripheral nerve microvascular endothelial cell; **RT** = room temperature; **SNAPC1** = small nuclear RNA activating complex polypeptide 1.

Introduction

Guillain-Barré syndrome (GBS) is an acute immune-mediated neuropathy characterized by rapidly progressive weakness of the extremities, occasional sometimes respiratory insufficiency (in approximately 25% of patients), and/or autonomic dysfunction after an antecedent infection.[1-4] Molecular mimicry of pathogen-borne antigens is considered the pathogenesis of GBS, and anti-glycolipid antibodies produced by the immune response after antecedent infection can cross-react with gangliosides at the nerve membrane.[2] The diagnosis is usually made based on clinical characteristics; however, findings of protein elevation in the CSF, presence of demyelination and/or axonal changes in a nerve conduction study, and the assay of anti-ganglioside autoantibodies can support the diagnosis of GBS and differentiate demyelinating from axonal subtypes.[5] *Campylobacter jejuni* is responsible for at least one-third of antecedent infections; however, other infections, including those caused by cytomegalovirus (CMV), Epstein-Barr virus (EBV), *Mycoplasma pneumoniae*, *Haemophilus influenzae*, influenza A virus, Zika virus, and hepatitis E virus, are also reportedly related to the pathogenesis of GBS.[6]

The disruption of the blood-nerve barrier (BNB) is critical for GBS development because the BNB functions as a barrier restricting the entry of humoral factors from blood into the peripheral nerve.[7,8] Several clinical findings suggest BNB abnormalities in cases of GBS, including an increase in the CSF/serum albumin quotient (Q-Alb), gadolinium enhancement of the lumbosacral nerve root on MRI, and the accumulation of inflammatory cells such as mononuclear leukocytes and monocytes around endoneurial microvessels on pathologic examinations.[9-11] However, the molecular mechanism underlying the BNB breakdown in GBS remains unclear, despite major advances in molecular biology.

This study assessed the contribution of serum IgG from individual patients with GBS to BNB impairment using human peripheral nerve microvascular endothelial cells (PnMECs) with RNA-seq, high-content imaging, and functional assays. We identified the U1-small nuclear ribonucleoprotein (U1-snRNP) autoantibodies responsible for initiating BNB breakdown in GBS.

Methods

Study Protocol Approvals, Registrations, and Patient Consents

The ethics committees of the Medical Faculties of Yamaguchi University approved this research (IRB# 2024-016). We obtained the written informed consent from each participant.

Patient IgG Samples

We collected serum samples from 77 patients with GBS in the acute phase after the onset of weakness and before treatment, all of whom had undergone medical examinations or were referred to Yamaguchi University Hospital for the assessment of the presence of serum anti-glycolipid antibodies. We also included serum samples from 24 healthy controls (HCs), 24 inflammatory disease controls (DCs) during the acute phase within 14 days of relapse before treatment (DC1s: multiple sclerosis, n = 14; neuromyelitis optica, n = 10), and 27 non-inflammatory DCs (DC2s: amyotrophic lateral sclerosis, n = 17; multiple system atrophy, n = 3; hereditary peripheral neuropathy, n = 2; cervical spondylosis, n = 2; spinocerebellar degeneration, n = 1; normal pressure hydrocephalus, n = 1; progressive supranuclear palsy, n = 1). Serum samples were stored at −80°C until the experiments. Before the experiments, the serum samples were inactivated (at 56°C, for 30 minutes). We prepared purified IgG from patient serum samples according to a Melon Gel IgG Spin Purification Kit (Thermo Fisher Scientific).

Clinical Information From Patients With GBS

We collected the following information from patients with GBS: sex, age, causative bacteria/virus for the antecedent infection (*C. jejuni*, CMV, EBV, *H. influenzae*, and *M. pneumoniae*),[12] anti-ganglioside antibodies (anti-GM1, GD1a, GalNAc-GD1a, GT1a, GQ1b IgG antibodies),[13] GBS Disability Scale (GDS) score on admission/peak, and ΔGDS score (peak GDS score-admission GDS score).

Immunohistochemistry of NF-κB in High-Content Imaging Assays

For all experiments, we used human PnMECs, specifically the FH-BNB cell line, which are immortalized human BNB-containing endothelial cells with a temperature-sensitive SV40 large T antigen and telomerase.[14] All experiments were conducted 2 days after the temperature was changed from 33 to 37°C.

The cells were maintained in the MCDB 131 medium containing 500 μg/mL of IgG from patients with GBS, DC1s, DC2s, or HCs with blind experiments on collagen type1–coated CELLSTAR 96-well plates (Greiner) after MCDB 131 medium substitution for 1 hour. Cells were fixed with 4% paraformaldehyde (PFA), permeabilized with 0.3% Triton X-100, and blocked overnight in 5% fetal bovine serum (FBS)/0.3% Triton X-100 in phosphate-buffered saline (PBS). The cells were incubated with NF-κB p65 monoclonal antibodies (Cell Signal Technology) and then with secondary antibodies (Alexa Fluor 488 anti-rabbit IgG [Thermo Fisher Scientific]).

For high-content imaging,[15] 5,000 cells/well were seeded in 96-well plates. After immunostaining, images per well were captured at ×20 with 4 fields of view (800–1,000 cells) using an In Cell Analyzer 2000 (GE Healthcare) and then evaluated using the In Cell Analyzer software program (Cytiva). Data were obtained from the mean values of 6 experiments.

Paracellular Permeability of 10-kDa Dextran

FH-BNB cells were cultured on 0.4-mm pore 24-well collagen-coated Transwell culture inserts (Corning) on the luminal side for 3 days at 33°C and for 2 days at 37°C. The cells were incubated with 500 μg/mL of individual IgG from patients with GBS (n = 19), DC1s (n = 10), DC2s (n = 10), or HCs (n = 12) for 24 hours at 37°C. After washing the cells, fluorescein isothiocyanate (FITC)-labeled 10-kDa dextran (1 mg/mL, Sigma-Aldrich) was incubated to the luminal chamber. After 40 minutes, 100 μL of the medium was moved from the abluminal chamber into 96-well plates. Fluorescence intensity at 490/520 nm (absorption/emission) was analyzed using a FlexStation 3 Multi-Mode microplate reader (Molecular Devices). Data were obtained from the mean value of 4 experiments.

RNA-seq and Pathway Analyses

Samples of 500 μg/mL of IgGs from 4 patients with GBS or 4 HCs were incubated for 12 hours with FH-BNB cells. RNA-seq and pathway analysis methods have been described (eFigure 1).[16] We normalized the mapped read counts to transcripts per million. We calculated p values with an unpaired Student t test and determined the fold-change (FC) by subtracting the average values of the HCs from those of patients with GBS for volcano plots. We used genes with a p value < 0.05 and a >50% change in FC for the ingenuity pathway analysis (IPA) to analyze the detected genes (Qiagen).

Immunohistochemistry of CXCR5, SNAPC1, NFAT, ICAM-1, snRNP, and Claudin-5 According to High-Content Imaging Assays

The methods used were almost the same as those used for NF-κB immunostaining. Cells (5,000 cells/well) were cultured in the MCDB 131 medium containing IgG (500 μg/mL) from patients with GBS (n = 22) or HCs (n = 7) in 96-well plates after MCDB 131 medium substitution for 24 hours for immunostaining of C-X-C chemokine receptor type 5 (CXCR5), small nuclear RNA activating complex polypeptide 1 (SNAPC1), nuclear factor of activated T cells (NFAT), intercellular adhesion molecule 1 (ICAM-1), snRNP, and claudin-5.

For CXCR5, SNAPC1, NFAT, ICAM-1, and snRNP, the cells were fixed with 4% PFA, permeabilized with 0.3% Triton X-100, and blocked overnight in 5% FBS/0.3% Triton X-100 in PBS. For ICAM-1, the cells were fixed with 4% PFA and blocked overnight in 5% FBS in PBS. For claudin-5, cells were fixed with 100% ethanol, permeabilized with 1% Triton X-100, and blocked overnight in 5% FBS/0.3% Triton X-100 in PBS.

The cells were incubated with primary monoclonal antibodies (CXCR5 [Abcam], SNAPC1 [Abcam], NFAT [Santa Cruz] or ICAM-1 [Santa Cruz], snRNP [Santa Cruz], and claudin-5 [Thermo Fisher Scientific]) and then with each secondary antibody (Alexa Fluor 488 anti-rabbit/mouse/goat IgG [Thermo Fisher Scientific]).

The images were analyzed using the In Cell Analyzer software program (Cytiva). Data were obtained from the mean value of 3 experiments for CXCR5, SNAPC1, NFAT, ICAM-1, snRNP, and claudin-5.

Detection of U1-snRNP Antibodies in Patients With GBS by ELISA

Serum samples from 77 patients with GBS, 16 HCs, 28 DCs, 26 patients with chronic inflammatory demyelinating polyradiculoneuropathy (CIDP) before treatments, 7 patients with acute disseminated encephalomyelitis (ADEM) within 14 days from onset, 18 patients with multiple sclerosis (AMS) of the acute phase within 14 days from relapse before treatment, 9 patients with secondary progressive MS, and 15 patients with neuromyelitis optica spectrum disorder (NMOSD) within 21 days before treatment were used for an ELISA (anti-RNP-70, RUO632, Sebia). Serum samples were tested according to the manufacturer's instructions. In brief, diluted serum samples and positive and negative control samples were placed in a 96-well plate coated with RNP-70. After 30 minutes of incubation at room temperature (RT) on a shaker, the well contents were discarded and washed 3 times. Next, the enzyme conjugate containing horseradish peroxidase (HRP)–labeled anti-human IgG antibodies was incubated for 15 minutes. After incubating tetramethylbenzidine substrate solution for 15 minutes, the stop solution was added. Well absorbance was measured at 450 nm using an ELISA plate reader (Molecular Devices). A calibration curve was constructed by plotting the calibrator concentration on the x-axis (log scale) against the absorbance of the calibrators on the y-axis (linear scale). We also included 4 samples from patients with GBS in the acute phase before IV immunoglobulin (IVIg) treatment, who were being treated with IVIg, and who had been in clinical remission for at least one month. Available clinical information including causative bacteria/virus for antecedent infection (*C. jejuni*, CMV, EBV,

H. influenzae, and *M. pneumoniae*), CSF protein level, IgG index, QALB/QALBLIM, and ΔGBS score was collected. Both QALB (CSF/serum albumin ratio) and QALBLIM [(age/15) + 4] were calculated for the functional assessment of blood–spinal nerve root barrier (B-SNR-B) permeability.[17]

Assessing for the Function of snRNP Antibodies Using an In Vitro BNB Model

Commercial snRNP Abs (sc-390899; Santa Cruz Biotechnology) and mouse polyclonal Abs (sc-2025; Santa Cruz Biotechnology) as a control IgG were used. We prepared GBS-IgG purified from 20 GBS patients with U1-snRNP antibodies and control-IgG from pooled 10 healthy individuals. To prepare the monolayer in vitro BNB coculture model, we maintained FH-BNB cells on the luminal side and human peripheral nerve pericytes on the abluminal side on Transwell culture inserts for 5 days (pore size: 0.4 mm, 24-well; Corning). To prepare spheroids, FH-BNB cells and human peripheral nerve pericytes were resuspended at 5,000 cells/microwell in a 1:1 ratio in a seeding volume of 100 μL per well (Cell-able). The cells were grown in a humidified incubator at 37°C in 5% CO_2 for 3 days to allow the self-assembly of multicellular organoids.

Cultured cells were incubated with this snRNP-Abs/cont-Abs (10 μg/mL) or GBS-IgG/cont-IgG (500 μg/mL) for 12 hours to evaluate the snRNP expression and permeability of 10-kDa dextran in the coculture model and to observe the claudin-5 expression and permeability of 10-kDa dextran in the spheroid model.

Three-lane organoplates with 400 μm × 220 μm (w × h) channels (Mimetas BV) were used to create microfluidic in vitro BNB coculture models.[18,19] After loading the cell suspension with human peripheral nerve pericyte (2.5×10^6 cells/mL) in collagen I gel (2 μL) into the middle channel, PnMECs were seeded and cultured in the top channel to establish a BNB microfluidic coculture model. CB medium and fresh Sciencell pericyte medium were used to assess their influence on barrier function. For the barrier integrity assay, 20 μL of the CB medium without fluorescence was added to the bottom-channel inlets and outlets. After the CB medium containing 0.5 mg/mL of FITC-dextran (20 kDa, FD20S, Sigma, St. Louis, MO) was added to the PnMEC microvessel in the top channel (40 μL on inlet; 30 μL on outlet), images were acquired. Fluorescent molecule leakage from the lumen of the microvessel to the adjacent middle channel was imaged using a BZ-X800 microscope (KEYENCE).

Knockdown of snRNP Using Small Interfering RNA

Cells were cultured at 37°C in a CO_2 incubator until 80% confluency. The cells were then transfected with snRNP siRNA (Santa Cruz) or control siRNA following the siRNA transfection protocol.

Immunoadsorption of U1-snRNP Antibody From GBS-IgG

We prepared GBS-IgG positive for anti-snRNP antibody purified from 20 GBS patients with U1-snRNP antibodies (U1-snRNP antibody–positive GBS-IgG), U1-snRNP antibody–negative GBS-IgG purified from 20 GBS patients without U1-snRNP antibodies, and HC-IgG from pooled 10 healthy individuals. U1-snRNP antibody–positive GBS-IgG was incubated on an ELISA plate with immobilized U1-snRNP for 2 hours at RT. We then collected the supernatant for subsequent analyses as GBS-IgG after the removal of the U1-snRNP antibody. The titer of U1-snRNP antibody is as follows: (1) U1-snRNP antibody–positive GBS-IgG 55 U/mL, (2) U1-snRNP antibody–negative GBS-IgG 10 U/mL, (3) GBS-IgG after removal of U1-snRNP antibody 20 U/mL, and (4) HC-IgG 2 U/mL.

Statistical Analyses

We used the Prism 7 software program (Graph Pad) to perform all statistical analyses. We used an unpaired Student *t* test (2-sided) for single comparison analyses, 1-way analysis of variance with the Tukey multiple comparisons test for multiple comparison analyses, and Pearson correlation coefficients for association assessments. $^{*}p < 0.05$, $^{**}p < 0.01$, and $^{***}p < 0.001$ were considered statistically significant.

Data Availability

Any data not provided in this article are available in anonymized form and can be shared by request from any qualified investigator. Sharing requires approval of a data transfer agreement by Yamaguchi University.

Results

IgGs From Patients With GBS Induced NF-κB Nuclear Translocation in BNB-Endothelial Cells

The experimental design of this study is illustrated in eFigure 2. First, we evaluated the number of NF-κB p65 nuclear translocations in FH-BNB among patients with GBS, DC1s (inflammatory controls), DC2s (noninflammatory controls), and HCs (Figure 1A). The percentage of NF-κB p65 nuclear–positive cells in the GBS group was significantly higher than in other groups (Figure 1A), with no marked difference in the percentage between infection controls and HCs (eFigure 3). Next, we compared the association between the proportion of nuclear NF-κB–positive cells and antecedent infections (caused by *C. jejuni*, CMV, EBV, *H. influenzae*, and *M. pneumoniae*) and serum anti-ganglioside antibodies (GM1, GD1a, GalNAc-GD1a, GT1a, and GQ1b) (Figure 1, B and C). IgG from GBS patients with antecedent infection with *C. jejuni*, *H. influenzae*, and *M. pneumoniae* or without the detection of an antecedent infection significantly increased NF-κB nuclear translocation in FH-BNB, compared with that from DC1s, DC2s, and HCs (Figure 1B). In addition, IgG from GBS patients with antibodies against GM1, GQ1b, or GT1a, or that from GBS patients without anti-ganglioside

Figure 1 NF-κB p65 Activation of Blood-Nerve Barrier (BNB)–Endothelial Cells after Exposure to IgG From Patients With Guillain-Barré Syndrome

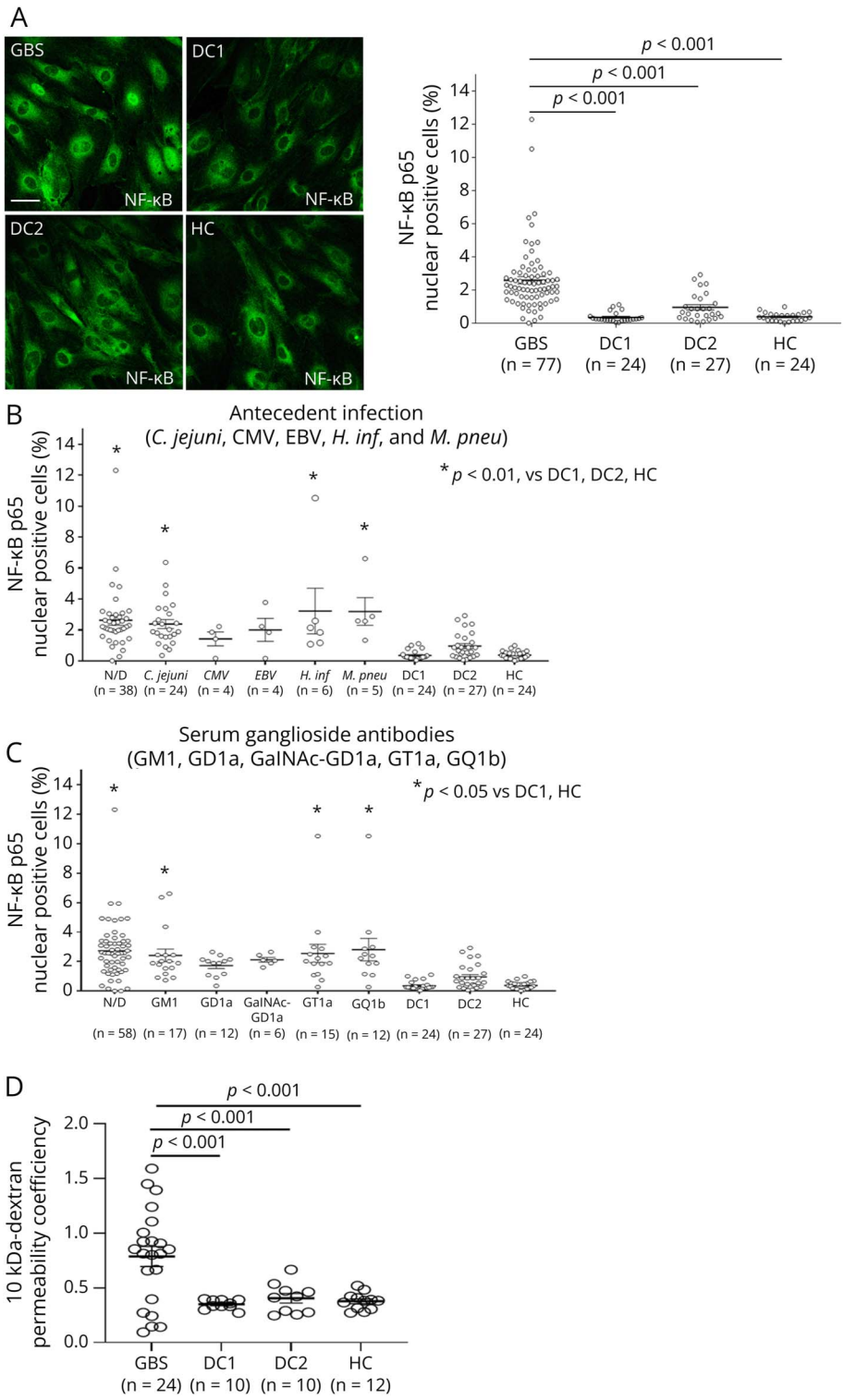

(A) Immunostaining of human peripheral nerve microvascular endothelial cells (PnMECs) for NF-κB p65 (green) after exposure to IgG (500 μg/mL) from patients with Guillain-Barré syndrome (GBS), inflammatory disease controls (DC1s), non-inflammatory disease controls (DC2s), or healthy controls (HCs). The images were captured using a confocal microscope. Scale bar, 50 μm. Scatter plots of the number of nuclear NF-κB p65–positive PnMECs, as determined using a high-content imaging system after exposure to IgG from patients with GBS (n = 77), DC1s (n = 24), DC2s (n = 27), and HCs (n = 24). The data were normalized to cultures that had not been exposed to human IgG and are shown as the mean ± SEM from 4 independent experiments, performed in triplicate. *p* values were determined using the Tukey multiple comparisons test. (B) Scatter plots of the number of nuclear NF-κB p65–positive PnMECs, as determined by high-content imaging, after exposure to IgG from GBS patients with antecedent infection with *Campylobacter jejuni* (*C. jejuni*: n = 24), CMV (n = 4), EBV (n = 4), *H. influenzae* (*H. influ*: n = 6), and *M. pneumoniae* (*M. pneu*: n = 4) or no antecedent infection detected (N/D, n = 38), DC1s (n = 24), DC2s (n = 27), and HCs (n = 24). The *p* values were determined by the Tukey multiple comparisons test (*$p < 0.01$, vs DC1, DC2, and HC groups). (C) Scatter plots of the number of nuclear NF-κB p65–positive PnMECs, as determined by high-content imaging, after exposure to IgG from GBS patients with antibodies against GM1, GD1a, GalNAc-GD1a, GT1a, and GQ1b and with no anti-ganglioside antibodies (N/D), DC1s, DC2s, and HCs. *p* values were determined by the Tukey multiple comparisons test (*$p < 0.05$, vs DC1 and HC groups). (D) The change in the 10-kDa dextran permeability coefficient in PnMECs was determined after exposure to IgG (500 μg/mL) from patients with GBS (n = 24), DC1s (n = 10), DC2s (n = 10), and HCs (n = 12). *p* values were determined using the Tukey multiple comparisons test. CMV = cytomegalovirus.

antibodies significantly increased the percentage of NF-κB nuclear translocations in FH-BNB compared with that from DC1s and HCs (Figure 1C). No association between the percentage of NF-κB nuclear–positive cells and the GDS score on admission/peak was observed (eFigure 4).

We then selected the top 24 GBS-IgGs with increasing effects on NF-κB and measured the permeability of 10-kDa dextran after exposure to these IgGs. Permeability was significantly increased after exposure to IgG from the GBS group compared with that from the other groups (Figure 1D).

Identification of an Altered Gene Expression in BNB-Endothelial Cells After Exposure to IgG From Patients With GBS Using RNA-seq

We selected IgG samples from 4 patients with GBS showing the strongest influence on the induction of NF-κB p65 nuclear translocation in FH-BNB cells for RNA-seq. To identify important signaling pathways, a whole transcriptome analysis with RNA-seq in FH-BNB cells was performed after exposure to IgG from patients with GBS (n = 4) and HCs (n = 4). Over 57,000 genes were detected in each sample, and heat maps showed that 156 genes were significantly upregulated (FC > 1.5; $p < 0.05$) between the patients with GBS (n = 4) and HC groups (n = 4) (eFigure 5). In the IPA network analysis of the upregulated genes in FH-BNB cells, RELA (NF-κB p65) was detected in the center of the network analysis and snRNP, RN7SKRNU1-4, RNU1-1, and RNU1-28P were upregulated after exposure to GBS-IgGs. snRNP was identified as an upstream gene of NF-κB, and CXCR5 was detected as a downstream molecule of NF-κB (eFigure 1).

Effect of IgGs From Patients With GBS on Expression of CXCR5, SNAPC1, snRNP, and Claudin-5 in BNB-Endothelial Cells

We observed changes in the amounts of proteins suggested by RNA-seq data, including CXCR5, SNAPC1, NFAT, ICAM-1, snRNP, and claudin-5, after incubation with IgGs from patients with GBS (Figure 2, A and B). A high content-imaging system showed that the expression of CXCR5 and SNAPC1 was significantly increased (Figure 2, A and B), whereas that of snRNP and claudin-5 was significantly decreased (Figure 2, A and B) in FH-BNB cells after incubation with IgGs from the GBS group compared with those from the HC group. The expression of NFAT and ICAM-1 was not markedly changed after exposure to IgG from patients with GBS or HCs (Figure 2, A and B).

Increase in U1-snRNP Autoantibodies in Patients With GBS

Our RNA-seq and pathway analyses showed upregulation of NF-κB signaling and identified snRNP as upstream of NF-κB in the GBS group. An evaluation with a high-content imaging system demonstrated a significant decrease in snRNP and a significant increase in NF-κB and SNAPC1 in patients with GBS compared with HCs. We hypothesized that U1-snRNP antibodies can be detected in patients with GBS and that these antibodies may induce the loss of U1-snRNP because these data suggest that the reduction of snRNP protein was an upstream signal mediating the breakdown of BNB. Titers of U1-snRNP antibodies were assayed in serum samples from patients with GBS or CIDP; DCs or HCs; and patients with ADEM, MS, NMOSD, and meningitis by an ELISA (Figure 3A). The rate of U1-snRNP antibody positivity was 36% (28/77) in patients with GBS, 7% (2/28) in DCs, 0% (0/16) in HCs, 0% (0/26) in patients with CIDP, 0% (0/10) in patients with meningitis, 0% (0/7) in patients with ADEM, 0% (0/18) in patients with AMS, 0% (0/9) in patients with secondary progrsessive multiple sclerosis (SPMS), 0% (0/15) in patients with NMOSD (Figure 3A). The cutoff value between positive and negative U1-snRNP antibodies was defined as the mean of HCs + 2SD (15U/L). The serum titer of snRNP antibody decreased before and after IVIg treatment (Figure 3B). The percentage of NF-κB nuclear–positive cells and 10-kDa dextran permeability efficiency in GBS-IgG–positive U1-snRNP antibodies were higher than those in GBS-IgG–negative U1-snRNP antibodies (Figure 3C). Both CSF protein and QALB/QALBLIM in snRNP antibody–positive GBS patients were increased compared with those in snRNP antibody–negative GBS patients (Figure 3C) while the IgG index and peak GDS scale showed no marked difference between the groups (eFigure 6). Antecedent infections in 28 cases of anti-snRNP antibody–positive GBS were caused by *C. jejuni* in 22% (6/28), CMV in 4% (1/28), EBV in 4% (1/28), and *H. influenzae* in 11% (3/28) (eFigure 7).

Effect of snRNP Antibodies on the Barrier Function of BNB Through U1-snRNP Reduction

GBS-IgG was purified from the serum samples of 20 patients with U1-snRNP autoantibody–positive GBS, and cont-IgG was purified from the serum samples of 10 HCs. Incubation with GBS-IgG with U1-snRNP antibodies or purified anti-snRNP antibody caused a decrease in nuclear snRNP expression in monolayer FH-BNB cells (Figure 4A) and a significant increase in 10-kDa dextran permeability (Figure 4B), compared with that with cont-IgG or cont-Ab, using a monolayer coculture model consisting of FH-BNB cells and pericytes. After transfection with snRNP siRNA, downregulation of snRNP increased the permeability of monolayer FH-BNB cells (eFigure 8). GBS-IgG with U1-snRNP antibody demonstrated a significant increase in the permeability of FH-BNB than cont-IgG, GBS-IgG without anti-U1-snRNP antibody, or GBS-IgG without U1-snRNP antibody after immunoabsorption of U1-snRNP antibody from GBS-IgG with U1-snRNP antibody (Figure 4C). No marked difference with complement-dependent cell death of PnMECs was observed among GBS-IgG with U1-snRNP antibody, GBS-IgG without U1-snRNP antibody, and cont-IgG (eFigure 9). Incubation with GBS-IgG or snRNP antibodies led to a decrease in claudin-5 and an increase in 10-kDa dextran permeability compared with cont-IgG using the spheroid model, which consists of both FH-BNB cells and pericytes (Figure 4D). Permeability of 20-kDa dextran was increased after exposure to GBS-IgG or snRNP antibodies compared with cont-IgG using microfluidic in vitro BNB coculture models (Figure 4D).

Discussion

C. jejuni is the most probable trigger of the axonal GBS, although the pathogenesis of demyelinating GBS (acute inflammatory demyelinating polyradiculoneuropathy [AIDP]) remains unclear.[1,6] Breakdown of the BNB in GBS first occurs at sites with weak BNB, such as the dorsal root ganglia and nerve terminals.[7] BNB disruption, which includes enhanced

Figure 2 Changes in the CXCR5, SNAPC1, NFAT, ICAM-1, U1-snRNP, and Claudin-5 After Exposure to IgG From Patients With GBS

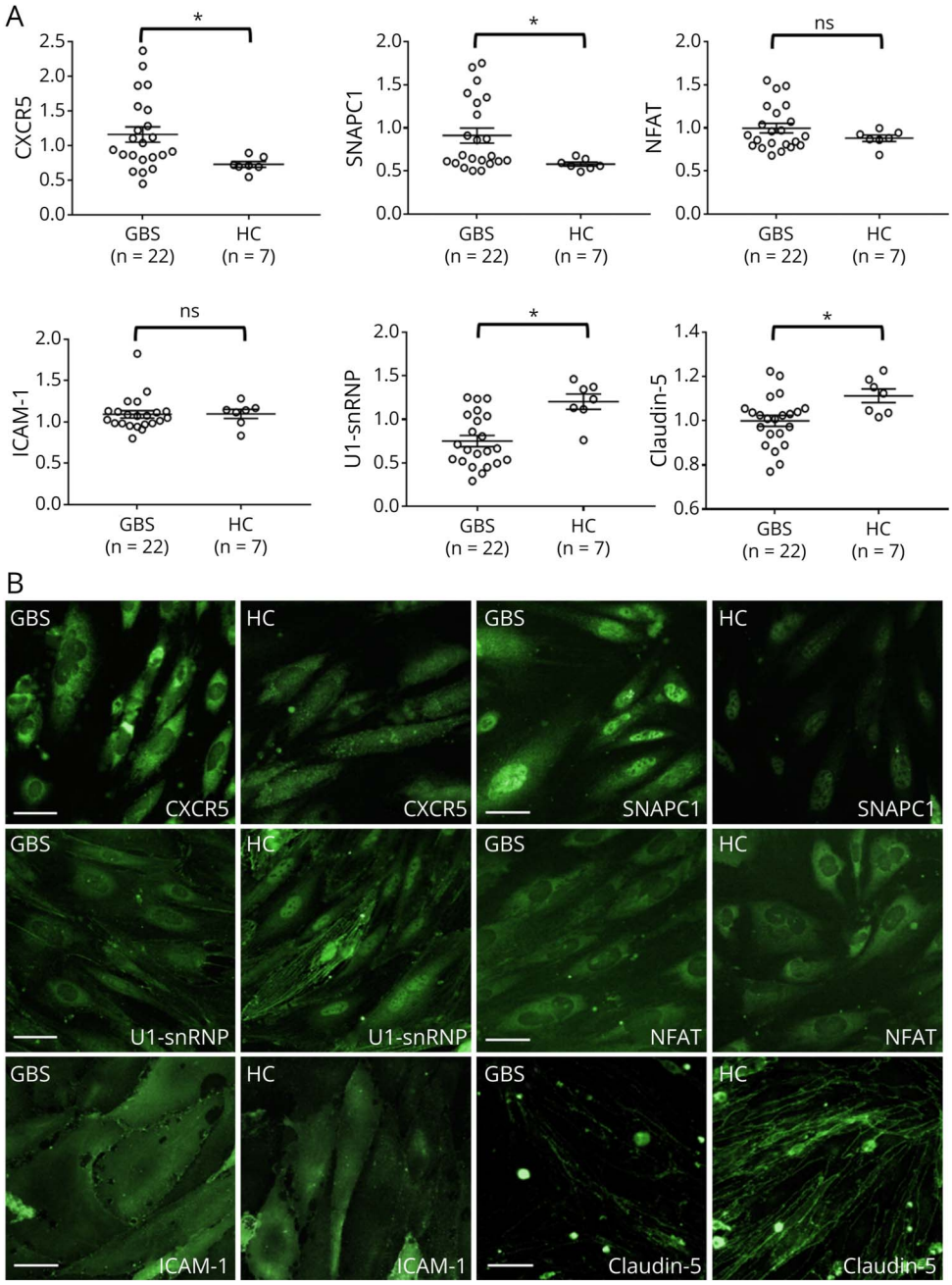

(A and B) Immunostaining of human peripheral nerve microvascular endothelial cells (PnMECs) for CXCR5, SNAPC1, NFAT, ICAM-1, U1-snRNP, and claudin-5 (green) after exposure to IgG (500 μg/mL) from patients with GBS or HCs. Images were captured using an In Cell Analyzer 2000. Scale bar, 50 μm. (A) Scatter plots of the intensities of CXCR5, SNAPC1, NFAT, ICAM-1, U1-snRNP, and claudin-5 in PnMECs, as determined by high-content imaging, after exposure to IgG from patients with GBS (n = 22) or HCs (n = 7). The data were normalized to cultures that had not been exposed to human IgG and are shown from 3 independent experiments. The p values were determined using an unpaired Student t test (2-sided) (*p < 0.05 vs HCs). CXCR5 = C-X-C chemokine receptor type 5; GBS = Guillain-Barré syndrome; ICAM-1 = intercellular adhesion molecule 1; NFAT = nuclear factor of activated T cells; PnMEC = peripheral nerve microvascular endothelial cell; SNAPC1 = small nuclear RNA activating complex polypeptide 1; U1-snRNP = U1-small nuclear ribonucleoprotein.

paracellular permeability and increased leukocyte trafficking through adhesion molecules and chemokines, is pathologically associated with GBS.[8,11,20] Pathologic findings of the peripheral nerves of patients with AIDP are characterized by monocyte predominance and less T-cell/B-cell infiltration into the peripheral nerve, suggesting the entry of macrophages across the BNB and macrophage-mediated demyelination.[11] Some in vitro BNB models have demonstrated that serum samples from patients with GBS enhance the leakage of small molecules in bovine PnMECs,[21] and an in vitro flow-based human BNB model has shown the importance of leukocyte integrin CD11b and ICAM-1 interactions in patients with GBS for leukocyte trafficking.[22] Furthermore, large clusters of endoneurial CD11b-positive leukocytes were observed in the sural nerve of patients with AIDP, and treatment with anti-CD11b antibody ameliorated disease severity in experimental autoimmune neuritis.[22-24]

In this study, we first demonstrated a significant increase in nuclear NF-κB–positive FH-BNB cells after exposure to IgG from patients with GBS compared with that obtained from DCs and HCs. IgGs from GBS patients with antecedent

Figure 3 U1-snRNP Autoantibodies in Patients With GBS

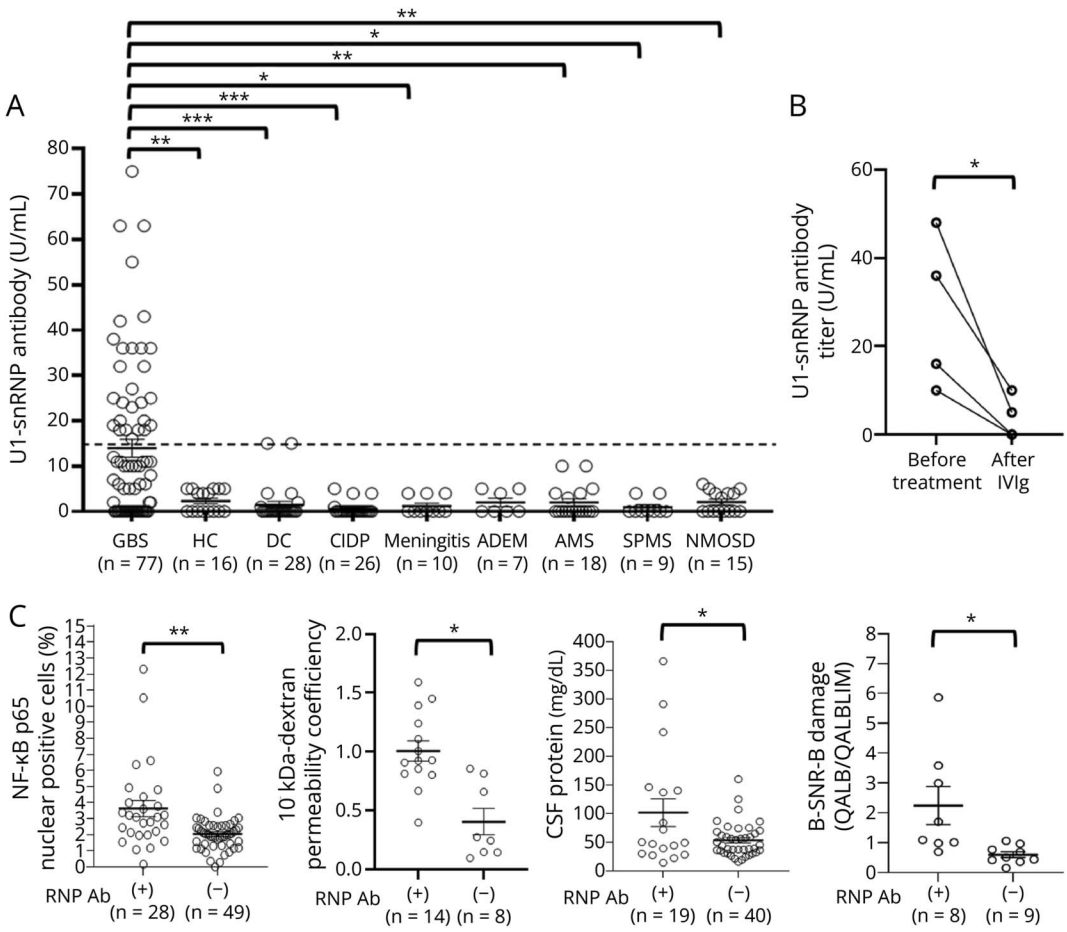

(A) Serum titers of U1-snRNP autoantibodies in patients with GBS were significantly increased compared with those in patients with CIDP, DCs, or HCs by an ELISA. The rate of U1-snRNP antibody positivity was 36% (28/77) in patients with GBS, 7% (2/28) in DCs, 0% (0/16) in HCs, 0% (0/26) in patients with CIDP, 0% (0/10) in patients with meningitis, 0% (0/7) in patients with ADEM, 0% (0/18) in patients with AMS, 0% (0/9) in patients with SPMS, and 0% (0/15) in patients with NMOSD. The dotted line indicates the positivity threshold (mean of healthy control serum samples + 2SD, 15U/L). (B) Serum titer of snRNP antibodies decreased after IVIg treatment. Negative conversion of U1-snRNP autoantibodies occurred in 3 of 4 GBS cases. (C) The percentage of NF-κB nuclear–positive cells and 10-kDa dextran permeability efficiency in GBS-IgG positive for U1-snRNP antibodies were higher than in GBS-IgG negative for U1-snRNP antibodies. CSF protein and QALB/QALBLIM in snRNP antibody–positive GBS patients were higher than those in snRNP antibody–negative GBS patients. ADEM = acute disseminated encephalomyelitis; CIDP = chronic inflammatory demyelinating polyradiculoneuropathy; DC = disease control; GBS = Guillain-Barré syndrome; HC = healthy control; NMOSD = neuromyelitis optica spectrum disorder; U1-snRNP = U1-small nuclear ribonucleoprotein.

infection of *C. jejuni, H. influenzae,* and *M. pneumoniae* significantly increased NF-κB nuclear translocation in FH-BNB cells compared with those from DCs and HCs. The permeability of small molecules in FH-BNB cells was significantly increased, and key tight junction protein claudin-5 was significantly decreased after exposure to IgG from patients with GBS compared with that from DCs and HCs. RNA-seq and pathway analyses demonstrated the upregulation of NF-κB signaling and CXCR5 in the GBS group and identified snRNA as an upstream gene of NF-κB. An evaluation with high-content imaging demonstrated a significant decrease in snRNP and a significant increase in chemokine receptors CXCR5 and SNAPC1 in patients with GBS compared with HCs. The titer of U1-snRNP autoantibodies was significantly higher in patients with GBS than in those with CIDP, meningitis, ADEM, MS, and NMOSD, DCs, and HCs. The positive rate of U1-snRNP antibodies was 36% (27/77), and the titer of U1-snRNP was reduced at 1 month later. GBS-IgG positive for U1-snRNP antibodies increased the percentage of NF-κB nuclear–positive cells and 10-kDa dextran permeability efficiency compared with those negative for U1-snRNP antibodies. Patients with U1-snRNP antibody–positive GBS showed more damage to B-SNR-B than patients with U1-snRNP antibody–negative GBS. Downregulation of U1-snRNP using siRNA increased the permeability of FH-BNB. GBS-IgG with U1-snRNP antibodies or anti-snRNP monoclonal antibody caused a decrease in nuclear snRNP expression in FH-BNB and an increase in permeability in monolayer/spheroid/microfluidic coculture models. GBS-IgG positive for U1-snRNP antibody demonstrated a significant increase in the permeability of FH-BNB compared with GBS-IgG negative for U1-snRNP antibody or GBS-IgG positive for U1-snRNP antibody after the reduction of U1-snRNP antibody. No marked complement-dependent cell

Figure 4 U1-snRNP Autoantibodies Disrupt the Blood-Nerve Barrier

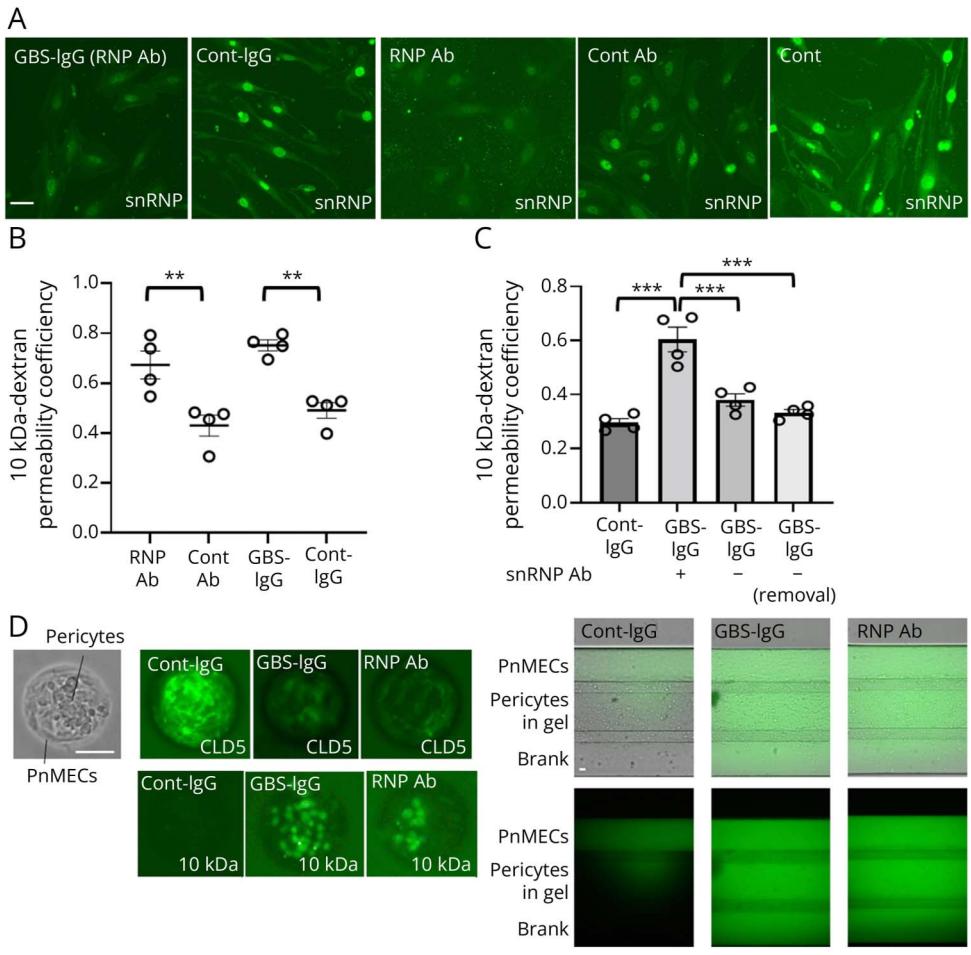

(A) Immunostaining of human peripheral nerve microvascular endothelial cells (PnMECs) for snRNPs. Nuclear snRNP expression in monolayer PnMECs decreased after incubation with GBS-IgG with snRNP antibodies or anti-snRNP monoclonal antibody compared with after cont-IgG or cont-Ab. GBS-IgG: IgG purified from serum samples of 20 patients with U1-snRNP autoantibody–positive GBS; cont-IgG: IgG purified from serum samples of 10 healthy controls; RNP antibody: commercial snRNP monoclonal antibody; cont-Ab: commercial anti-rabbit IgG. Scale bar, 50 μm. (B) Incubation of GBS-IgG with snRNP antibodies or anti-snRNP antibody caused a significant increase in 10-kDa dextran permeability, compared with that with cont-IgG or cont-Ab, using a monolayer coculture model consisting of FH-BNB cells and pericytes. (C) GBS-IgG with anti-snRNP antibody induced a significant increase in the permeability of FH-BNB compared with cont-IgG, GBS-IgG without anti-snRNP antibody, or GBS-IgG after the reduction of U1-snRNP antibody from GBS-IgG with U1-snRNP antibody. (D) Incubation with GBS-IgG or snRNP antibodies leads to a decrease in claudin-5 and an increase in 10-kDa dextran permeability compared with cont-IgG using the spheroid model, which consists of both FH-BNB cells and pericytes (Left). Scale bar, 50 μm. Permeability of 20-kDa dextran increased after exposure to GBS-IgG or snRNP antibodies compared with cont-IgG using a microfluidic in vitro BNB coculture model (Right). Scale bar, 100 μm. BNB = blood-nerve barrier; U1-snRNP = U1-small nuclear ribonucleoprotein.

death of PnMECs was observed after exposure to GBS-IgG with U1-snRNP antibody.

CXCR5 is the G-protein coupled receptor against the chemokine C-X-C motif ligand 13 (CXCL13) and is expressed on mature B lymphocytes,[25] $CD4^+$ follicular helper T cells (Tfh), $CD4^+$ Th17 cells,[26] and a minor subset of $CD8^+$ T cells.[27] CXCL13 is constitutively expressed in macrophages.[28] Our results suggest that CXCR5 on BNB-endothelial cells induced by GBS-IgG may play a role in the recruitment of CXCL13-positive macrophages and promote the infiltration of macrophages into the peripheral nervous system across the BNB in patients with GBS, supported by pathologic observations of macrophage-mediated demyelination. No reports have suggested an association between the CXCR5-CXCL13 axis and GBS.

The snRNP plays an important role as a spliceosome that removes introns from messenger RNA precursors, resulting in the production of mRNA.[29] SNAP1 plays an important role as a basal transcription factor that mediates the transcription of snRNAs.[30] Although the precise mechanism of SNAPC1 remains unclear, a recent report indicated its role as a general transcriptional coactivator that functions by elongating RNA polymerase II.[31] Our data suggest that GBS-IgG decreases U1-snRNP and increases SNAPC1 in FH-BNB cells, indicating that the expression of SNAPC1 was upregulated in response to the decrease in U1-snRNP after exposure to GBS-IgG in FH-BNB cells. Recent data suggest that reduced amounts of U1-snRNP activate the cell status of cancer cells and stimulate cancer cell migration and invasion in vitro,[32] although the influence of the reduction in U1-snRNP activity on BNB-endothelial cells remains unclear. In this study, the change in snRNPs caused the upregulation of the NF-κB p65 signaling with a pathway analysis and the downregulation of U1-snRNP, suggesting that a reduction in U1-snRNP after GBS-IgG exposure may initiate NF-κB signaling in FH-BNB cells as the upstream regulator. Furthermore, snRNP knockdown using siRNA increased the BNB permeability. Modulation of U1-snRNP may be a novel treatment target for GBS.

U1-snRNP autoantibodies have been reported in serum samples from patients with systemic lupus erythematosus, systemic sclerosis, mixed connective tissue disease (MCTD), or myositis, and snRNP antibody positivity has been clinically used to diagnose MCTD.[5,33,34] However, the exact roles of these antibodies in the pathogenesis of these diseases remain unclear. Some reports have shown that snRNP antibodies are related to the manifestations of microvasculopathy including Raynaud phenomenon, suggesting that snRNP antibodies can trigger inflammation in endothelial cells in patients with connective disease.[35,36] An in vitro study demonstrated that U1-RNP antibodies can bind to U1-RNP on the surface of endothelial cells from the pulmonary artery and induce inflammation in endothelial cells through upregulation of ICAM-1 and E-selectin.[35,37] In our study, U1-snRNP autoantibodies in patients with GBS led to BNB-endothelial cell dysfunction through the downregulation of snRNP and upregulation of NF-κB activation, resulting in increased permeability of the BNB in GBS.

Some reports suggest that viral infections, including those caused by CMV, HHV-6, HHV-7, HIV, and COVID-19, can trigger the production of U1-snRNP autoantibodies through molecular mimicry.[38-41] In particular, animal studies have shown that the molecular mimicry between epitopes in CMV glycoprotein B (amino acids 700–907) and charged amino acids to the carboxy terminal region of the U1-70K component of U1-snRNP may be responsible for the induction of the autoantibody response to U1-snRNP.[39] HHV-6, HHV-7, and EBV also have homologous glycoprotein B proteins with CMV.[39] The present study showed that antecedent infections with *C. jejuni*, CMV, and EBV are specifically related to GBS and have been identified as antecedent infections in cases of anti-U1-snRNP antibody–positive GBS. A temporary autoantibody response against snRNP could be boosted by the periodic response to viral infection in GBS, and such individuals may be at risk of developing GBS in a relative short period. A temporary increase in U1-snRNP antibodies was observed in the acute phase of patients with GBS in our study, which could be related to a spontaneous postinfectious antibody response or a therapeutic decrease related to treatment.

The deposition of complement has been implicated in patients with GBS: the deposition of C3d or both C3d and C5b-9 along the outer surface of the Schwann cells in the endoneurium was observed in both the autopsied nerves and biopsied nerves from patients with GBS.[42,43] However, no deposition of complement in BNB-endothelial cells has been previously reported in the peripheral nerves of patients with GBS. Our in vitro study also demonstrated no association between complement-dependent cell death of BNB-endothelial cells after the binding of U1-snRNP antibodies. By contrast, the deposition of complement C3 and IgM in the endoneurial blood vessels was observed in the sural nerve of patients with CIDP, thus possibly suggesting an association between breakdown of the BNB induced by complement in some patients with CIDP.[44,45] Clinical trials for complement inhibitors in GBS (NCT04701164) and CIDP (NCT04658472) are currently ongoing.

Limitations of this study are that the detailed mechanism by how anti-U1-snRNP antibodies can reach the nucleus remains unclear. Because what antecedent infection is associated with the production of U1-snRNP antibodies or which subtypes of GBS (AIDP or axonal GBS) are associated with U-snRNP antibody–positive GBS remains elusive, multicenter blinded studies are required.

In conclusion, this study shows that GBS-IgG disrupts the BNB through increased permeability and CXCR5 upregulation. The rate of U1-snRNP antibody positivity was 36% in patients with GBS, and these antibodies cause BNB breakdown through a reduction in U1-snRNP and induction of NF-κB activation.

Author Contributions

F. Shimizu: drafting/revision of the manuscript for content, including medical writing for content; major role in the acquisition of data; study concept or design; analysis or interpretation of data. M. Koga: drafting/revision of the manuscript for content, including medical writing for content; analysis or interpretation of data. Y. Mizukami: analysis or interpretation of data. K. Watanabe: analysis or interpretation of data. R. Sato: analysis or interpretation of data. Y. Takeshita: analysis or interpretation of data. T. Maeda: analysis or interpretation of data. T. Kanda: analysis or interpretation of data. M. Nakamori: drafting/revision of the manuscript for content, including medical writing for content; study concept or design.

Study Funding

Funding organizations had no role in the design or conduct of this research. This research was supported by research grants (Nos. 24K10621, 21K07416 and 20H00529) from the Japan Society for the Promotion of Science, Tokyo, Japan, Grants for research on intractable diseases (Neuroimmunologic Disease Research Committee) from the Ministry of Health, Labour and Welfare of Japan, Chugai Foundation for Innovation Drug Discovery Science and Life Science Foundation of JAPAN.

Disclosure

The authors report no relevant disclosures. Full disclosure form information provided by the authors is available with the full text of this article at Neurology.org/NN.

Publication History

Received by *Neurology® Neuroimmunology & Neuroinflammation* October 15, 2024. Accepted in final form March 11, 2025. Submitted and externally peer reviewed. The handling editor was Marinos C. Dalakas, MD, FAAN.

References

1. Willison HJ, Jacobs BC, van Doorn PA. Guillain-Barré syndrome. *Lancet* 2016; 388(10045):717-727. doi:10.1016/S0140-6736(16)00339-1

2. van den Berg B, Walgaard C, Drenthen J, Fokke C, Jacobs BC, van Doorn PA. Guillain-Barré syndrome: pathogenesis, diagnosis, treatment and prognosis. *Nat Rev Neurol*. 2014;10(8):469-482. doi:10.1038/nrneurol.2014.121
3. Esposito S, Longo MR. Guillain-Barré syndrome. *Autoimmun Rev*. 2017;16(1):96-101. doi:10.1016/j.autrev.2016.09.022
4. Doets AY, Jacobs BC, van Doorn PA. Advances in management of Guillain-Barré syndrome. *Curr Opin Neurol*. 2018;31(5):541-550. doi:10.1097/WCO.0000000000000602
5. Chevalier K, Chassagnon G, Leonard-Louis S, et al. Anti-U1RNP antibodies are associated with a distinct clinical phenotype and a worse survival in patients with systemic sclerosis. *J Autoimmun*. 2024;146:103220. doi:10.1016/j.jaut.2024.103220
6. Hughes RAC. Guillain-Barré syndrome: history, pathogenesis, treatment, and future directions. *Eur J Neurol*. 2024;31(11):e16346. doi:10.1111/ene.16346
7. Kanda T. Biology of the blood-nerve barrier and its alteration in immune mediated neuropathies. *J Neurol Neurosurg Psychiatry*. 2013;84(2):208-212. doi:10.1136/jnnp-2012-302312
8. Ubogu EE. Biology of the human blood-nerve barrier in health and disease. *Exp Neurol*. 2020;328:113272. doi:10.1016/j.expneurol.2020.113272
9. Gorson KC, Ropper AH, Muriello MA, Blair R. Prospective evaluation of MRI lumbosacral nerve root enhancement in acute Guillain-Barré syndrome. *Neurology*. 1996;47(3):813-817. doi:10.1212/wnl.47.3.813
10. Wang XK, Zhang HL, Meng FH, et al. Elevated levels of S100B, tau and pNFH in cerebrospinal fluid are correlated with subtypes of Guillain-Barré syndrome. *Neurol Sci*. 2013;34(5):655-661. doi:10.1007/s10072-012-1092-z
11. Ubogu EE. Inflammatory neuropathies: pathology, molecular markers and targets for specific therapeutic intervention. *Acta Neuropathol*. 2015;130(4):445-468. doi:10.1007/s00401-015-1466-4
12. Koga M, Gilbert M, Li J, et al. Antecedent infections in Fisher syndrome: a common pathogenesis of molecular mimicry. *Neurology*. 2005;64(9):1605-1611. doi:10.1212/01.WNL.0000160399.08456.7C
13. Koga M, Takahashi M, Yokoyama K, Kanda T. Ambiguous value of anti-ganglioside IgM autoantibodies in Guillain-Barré syndrome and its variants. *J Neurol*. 2015;262(8):1954-1960. doi:10.1007/s00415-015-7806-4
14. Abe M, Sano Y, Maeda T, et al. Establishment and characterization of human peripheral nerve microvascular endothelial cell lines: a new in vitro blood-nerve barrier (BNB) model. *Cell Struct Funct*. 2012;37(2):89-100. doi:10.1247/csf.11042
15. Shimizu F, Takeshita Y, Sano Y, et al. GRP78 antibodies damage the blood-brain barrier and relate to cerebellar degeneration in Lambert-Eaton myasthenic syndrome. *Brain*. 2019;142(8):2253-2264. doi:10.1093/brain/awz168
16. Kohno M, Kobayashi S, Yamamoto T, et al. Enhancing calmodulin binding to cardiac ryanodine receptor completely inhibits pressure-overload induced hypertrophic signaling. *Commun Biol*. 2020;3(1):714. doi:10.1038/s42003-020-01443-w
17. Ruiz M, Puthenparampil M, Campagnolo M, et al. Oligoclonal IgG bands in chronic inflammatory polyradiculoneuropathies. *J Neurol Neurosurg Psychiatry*. 2021;92(9):969-974. doi:10.1136/jnnp-2020-325868
18. Wevers NR, Kasi DG, Gray T, et al. A perfused human blood-brain barrier on-a-chip for high-throughput assessment of barrier function and antibody transport. *Fluids Barriers CNS*. 2018;15(1):23. doi:10.1186/s12987-018-0108-3
19. Ohbuchi M, Shibuta M, Tetsuka K, et al. Modeling of blood-brain barrier (BBB) dysfunction and immune cell migration using human BBB-on-a-Chip for Drug Discovery research. *Int J Mol Sci*. 2024;25(12):6496. doi:10.3390/ijms25126496
20. Stubbs EB Jr. Targeting the blood-nerve barrier for the management of immune-mediated peripheral neuropathies. *Exp Neurol*. 2020;331:113385. doi:10.1016/j.expneurol.2020.113385
21. Kanda T, Yamawaki M, Mizusawa H. Sera from Guillain-Barré patients enhance leakage in blood-nerve barrier model. *Neurology*. 2003;60(2):301-306. doi:10.1212/01.wnl.0000041494.70178.17
22. Yosef N, Ubogu EE. α(M)β(2)-integrin-intercellular adhesion molecule-1 interactions drive the flow-dependent trafficking of Guillain-Barré syndrome patient derived mononuclear leukocytes at the blood-nerve barrier in vitro. *J Cel Physiol*. 2012;227(12):3857-3875. doi:10.1002/jcp.24100
23. Dong C, Palladino SP, Helton ES, Ubogu EE. The pathogenic relevance of α_M-integrin in Guillain-Barré syndrome. *Acta Neuropathol*. 2016;132(5):739-752. doi:10.1007/s00401-016-1599-0
24. Liu S, Dong C, Ubogu EE. Immunotherapy of Guillain-Barré syndrome. *Hum Vaccin Immunother*. 2018;14(11):2568-2579. doi:10.1080/21645515.2018.1493415
25. Legler DF, Loetscher M, Roos RS, Clark-Lewis I, Baggiolini M, Moser B. B cell-attracting chemokine 1, a human CXC chemokine expressed in lymphoid tissues, selectively attracts B lymphocytes via BLR1/CXCR5. *J Exp Med*. 1998;187(4):655-660. doi:10.1084/jem.187.4.655
26. Lim HW, Lee J, Hillsamer P, Kim CH. Human Th17 cells share major trafficking receptors with both polarized effector T cells and FOXP3+ regulatory T cells. *J Immunol*. 2008;180(1):122-129. doi:10.4049/jimmunol.180.1.122
27. Lim HW, Hillsamer P, Kim CH. Regulatory T cells can migrate to follicles upon T cell activation and suppress GC-Th cells and GC-Th cell-driven B cell responses. *J Clin Invest*. 2004;114(11):1640-1649. doi:10.1172/JCI22325
28. Bellamri N, Viel R, Morzadec C, et al. TNF-A and IL-10 control CXCL13 expression in human macrophages. *J Immunol*. 2020;204(9):2492-2502. doi:10.4049/jimmunol.1900790
29. Krausová M, Staněk D. snRNP proteins in health and disease. *Semin Cel Dev Biol*. 2018;79:92-102. doi:10.1016/j.semcdb.2017.10.011
30. Bai L, Wang Z, Yoon JB, Roeder RG. Cloning and characterization of the beta subunit of human proximal sequence element-binding transcription factor and its involvement in transcription of small nuclear RNA genes by RNA polymerases II and III. *Mol Cel Biol*. 1996;16(10):5419-5426. doi:10.1128/MCB.16.10.5419
31. Baillat D, Gardini A, Cesaroni M, Shiekhattar R. Requirement for SNAPC1 in transcriptional responsiveness to diverse extracellular signals. *Mol Cel Biol*. 2012;32(22):4642-4650. doi:10.1128/MCB.00906-12
32. Oh JM, Venters CC, Di C, et al. U1 snRNP regulates cancer cell migration and invasion in vitro. *Nat Commun*. 2020;11:1. doi:10.1038/s41467-019-13993-7
33. Elhani I, Khoy K, Mariotte D, et al. The diagnostic challenge of patients with anti-U1-RNP antibodies. *Rheumatol Int*. 2023;43(3):509-521. doi:10.1007/s00296-022-05161-w
34. Casal-Dominguez M, Pinal-Fernandez I, Corse AM, et al. Muscular and extramuscular features of myositis patients with anti-U1-RNP autoantibodies. *Neurology*. 2019;92(13):e1416-e1426. doi:10.1212/WNL.0000000000007188
35. Okawa-Takatsuji M, Aotsuka S, Uwatoko S, et al. Endothelial cell-binding activity of anti-U1-ribonucleoprotein antibodies in patients with connective tissue diseases. *Clin Exp Immunol*. 2001;126(2):345-354. doi:10.1046/j.1365-2249.2001.01669.x
36. Todoroki Y, Kubo S, Nakano K, et al. Nailfold microvascular abnormalities are associated with a higher prevalence of pulmonary arterial hypertension in patients with MCTD. *Rheumatology (Oxford)*. 2022;61(12):4875-4884. doi:10.1093/rheumatology/keac165
37. Okawa-Takatsuji M, Aotsuka S, Fujinami M, Uwatoko S, Kinoshita M, Sumiya M. Up-regulation of intercellular adhesion molecule-1 (ICAM-1), endothelial leucocyte adhesion molecule-1 (ELAM-1) and class II MHC molecules on pulmonary artery endothelial cells by antibodies against U1-ribonucleoprotein. *Clin Exp Immunol*. 1999;116(1):174-180. doi:10.1046/j.1365-2249.1999.00864.x
38. Newkirk MM, van Venrooij WJ, Marshall GS. Autoimmune response to U1 small nuclear ribonucleoprotein (U1 snRNP) associated with cytomegalovirus infection. *Arthritis Res*. 2001;3(4):253-258. doi:10.1186/ar310
39. Curtis HA, Singh T, Newkirk MM. Recombinant cytomegalovirus glycoprotein gB (UL55) induces an autoantibody response to the U1-70 kDa small nuclear ribonucleoprotein. *Eur J Immunol*. 1999;29(11):3643-3653. doi:10.1002/(SICI)1521-4141(199911)29:11<3643::AID-IMMU3643>3.0.CO;2-J
40. Son K, Jamil R, Chowdhury A, et al. Circulating anti-nuclear autoantibodies in COVID-19 survivors predict long COVID symptoms. *Eur Respir J*. 2023;61(1):2200970. doi:10.1183/13993003.00970-2022
41. Zandman-Goddard G, Shoenfeld Y. HIV and autoimmunity. *Autoimmun Rev*. 2002;1(6):329-337. doi:10.1016/s1568-9972(02)00086-1
42. Hafer-Macko C, Hsieh ST, Li CY, et al. Acute motor axonal neuropathy: an antibody-mediated attack on axolemma. *Ann Neurol*. 1996;40(4):635-644. doi:10.1002/ana.410400414
43. Koike H, Fukami Y, Nishi R, et al. Ultrastructural mechanisms of macrophage-induced demyelination in Guillain-Barré syndrome. *J Neurol Neurosurg Psychiatry*. 2020;91(6):650-659. doi:10.1136/jnnp-2019-322479
44. Dalakas MC, Engel WK. Immunoglobulin and complement deposits in nerves of patients with chronic relapsing polyneuropathy. *Arch Neurol*. 1980;37(10):637-640. doi:10.1001/archneur.1980.00500590061010
45. Querol LA, Hartung HP, Lewis RA, et al. The role of the complement system in chronic inflammatory demyelinating polyneuropathy: implications for complement-targeted therapies. *Neurotherapeutics*. 2022;19(3):864-873. doi:10.1007/s13311-022-01221-y